Molecular Microbiology (2014) 93(4), 698–712 ■
doi:10.1111/mmi.12685
First published online 16 July 2014

A vacuolar-H$^+$-pyrophosphatase (TgVP1) is required for microneme secretion, host cell invasion, and extracellular survival of *Toxoplasma gondii*

Jing Liu,[1,2] Douglas Pace,[1†] Zhicheng Dou,[3] Thayer P. King,[1] Daniel Guidot,[1] Zhu-Hong Li,[1] Vern B. Carruthers[3] and Silvia N. J. Moreno[1*]

[1]*Center for Tropical and Emerging Global Diseases and Department of Cellular Biology, University of Georgia, GA 30602-7400, USA.*

[2]*College of Veterinary Medicine, China Agricultural University, Beijing 100193, China.*

[3]*Department of Microbiology & Immunology, University of Michigan Medical School, Ann Arbor, MI 48109-5620, USA.*

Summary

The vacuolar proton pyrophosphatase (H$^+$-PPase) of *Toxoplasma gondii* (TgVP1), a membrane proton pump, localizes to acidocalcisomes and a novel lysosome-like compartment termed plant-like vacuole (PLV) or vacuolar compartment (VAC). We report the characterization of a *T. gondii null* mutant for the *TgVP1* gene. Propagation of these mutants decreased significantly because of deficient attachment and invasion of host cells, which correlated with deficient microneme secretion. Processing of cathepsin L (CPL) in these mutants was deficient only when the parasites were incubated in the presence of low concentrations of the vacuolar H$^+$-ATPase (V-H$^+$-ATPase) inhibitor bafilomycin A$_1$, suggesting that either TgVP1 or the *T. gondii* V-H$^+$-ATPase (TgVATPase) are sufficient to support CPL processing. The lack of TgVP1 did not affect processing of micronemal proteins, indicating that it does not contribute to proMIC maturations. The *TgVP1 null* mutants were more sensitive to extracellular conditions and were less virulent in mice. We demonstrate that *T. gondii* tachyzoites possess regulatory volume decrease capability during hypo-osmotic stress and this ability is impaired in *TgVP1 null* mutants implicating TgVP1 in osmoregulation. We hypothesize that osmoregulation is needed for host cell invasion and that TgVP1 plays a role during the normal lytic cycle of *T. gondii*.

Accepted 19 June, 2014. *For correspondence. E-mail smoreno@uga.edu; Tel. (+1) 706 542 4736; Fax (+1) 706 542 9493. †Present address: California State University, Long Beach, CA, USA. No conflict of interest to declare from any of the authors.

Introduction

Toxoplasma gondii is a protist parasite that has emerged as a major opportunistic pathogen in people with deficient immune systems. Infection with *T. gondii* is usually asymptomatic and results in the formation of dormant bradyzoites that infect the brain and other tissues for life. The developing fetus and the immunosuppressed patients are at substantial risk of severe disease. The tachyzoite is the rapidly growing asexual form that is seen in acutely infected animals. Tachyzoites enter host cells by a process of active invasion, they replicate inside the cell and, after a certain number of replications exit to infect neighbouring cells. While searching for a host cell to invade, the parasite is exposed to an environment with an ionic composition quite different from the host intracellular composition. This sharp change from intracellular to extracellular milieu must pose a challenge to the fitness of the parasite, which needs to glide, extrude its conoid and secrete proteins from apical secretory organelles (micronemes and rhoptries) during invasion to form the moving junction and the parasitophorous vacuole for its next intracellular life.

Membrane pyrophosphatases couple pyrophosphate (PP_i) hydrolysis to the active transport of sodium or protons against an electrochemical gradient. Proton pyrophosphatases (H$^+$-PPases) are present in prokaryotes (Baltscheffsky *et al.*, 1966; Serrano *et al.*, 2007) and some eukaryotes including plants (Maeshima, 2000; Drozdowicz and Rea, 2001) and protists (Scott *et al.*, 1998; Marchesini *et al.*, 2000; Rodrigues *et al.*, 2000; McIntosh *et al.*, 2001; Drozdowicz *et al.*, 2003), but are absent in mammalian cells.

H$^+$-PPases are also called vacuolar PPases because they are preferentially localized in vacuolar compartments, like the plant vacuole (Maeshima, 2000), and acidocalcisomes of bacteria (Seufferheld *et al.*, 2003; 2004) and protists (Docampo and Moreno, 2011). In contrast to the multisubunit vacuolar H$^+$-ATPases (V-H$^+$-ATPases), H$^+$-PPases form homodimers (Maeshima, 2000) and are

divided in K^+-dependent and K^+-independent subfamilies (Belogurov and Lahti, 2002). A single amino acid near the cytoplasm–membrane interface, which is an Ala in the K^+-dependent and Lys in the K^+-independent enzymes (Belogurov and Lahti, 2002), is responsible for this dependence. All membrane H^+-PPases require Mg^{2+} for activity (Baykov *et al*., 1993) and the three dimensional structure of a H^+-PPase (Lin *et al*., 2012) has recently been reported. In prokaryotes, H^+-PPases have roles in generating an ion-motive force for ATP synthesis and transport of metabolites (Baltscheffsky *et al*., 1999; Garcia-Contreras *et al*., 2004; Lopez-Marques *et al*., 2004), while in eukaryotes they acidify intracellular organelles (Maeshima, 2000; Docampo and Moreno, 2011). Overexpression of H^+-PPase in plants confers resistance to water/nutrient deprivation, cold, and salinity (Park *et al*., 2005; Lv *et al*., 2008; Zhang *et al*., 2011), while loss of H^+-PPase leads to root and shoot growth defects (Li *et al*., 2005), which are related to its role in auxin transport and organ development. Downregulation of expression of the H^+-PPase of *Trypanosoma brucei* affects acidification of acidocalcisomes and growth of procyclic and bloodstream stages *in vitro* (Lemercier *et al*., 2002).

We recently discovered a novel multi-vesicular post-Golgi organelle in *T. gondii* tachyzoites termed the plant-like vacuole (PLV, the abbreviation used hereafter) (Miranda *et al*., 2010) or vacuolar compartment (VAC) (Parussini *et al*., 2010). This organelle can be labelled with antibodies against proteins with similarity to vacuolar plant pumps and channels, such as a K^+-sensitive H^+-PPase (TgVP1), and a tonoplast-like aquaporin (TgAQP1). Our results showed that the PLV becomes mostly evident during the extracellular stage of the parasite. Our hypothesis is that the TgVP1 present in the PLV is important for parasite survival under extracellular stress and preparation for invasion of host cells. We report the phenotypic analysis of *TgVP1 null* mutants with the aim of understanding the role of this prominent organelle in extracellular *T. gondii* tachyzoites.

Results

Targeting of TgVP1 and complementation

To define the role of TgVP1 in the life cycle of *T. gondii*, we generated knockout mutants (Δ*vp1*) by targeting the native *TgVP1* locus in the Δ*ku80* strain, which favours homologous recombination (Fox *et al*., 2009; Huynh and Carruthers, 2009). We used a cosmid-based recombineering approach (Brooks *et al*., 2010), as described under *Experimental procedures*. Successful gene deletion (Fig. 1A) was confirmed by Southern blot analysis (Fig. 1B, Δ*vp1*). Western blot analysis using affinity-purified antibody against TgVP1, and antibody against tubulin as loading control, showed lack of expression of the *TgVP1* gene (Fig. 1C, Δ*vp1*). The absence of expression of TgVP1 was also verified by immunofluorescence analysis (IFA) of Δ*vp1* cells with the same anti-TgVP1 antibody (Fig. 1D). IFA with an affinity-purified antibody against *T. gondii* cathepsin L (CPL) shows labelling of the PLV (Fig. 1D, white arrow) in Δ*vp1* (Fig. 1D, red), and Δ*ku80* (Fig. 1E, green) parasites. Restoration of gene expression was accomplished by transforming Δ*vp1* with a cosmid that contains the entire *TgVP1* genomic locus. Re-expression of *TgVP1* in the complemented clones (Δ*vp1-cm1*, Δ*vp1-cm2* and Δ*vp1-cm3*) appeared to be at appropriate levels, especially with Δ*vp1-cm1* (Fig. 1C), which was used for further experiments and termed Δ*vp1-cm* hereafter. IFA staining of tachyzoites confirmed re-expression of *TgVP1* in the PLV of clone Δ*vp1-cm* (Fig. 1E, red).

TgVP1 is required for efficient attachment and invasion of tachyzoites

We compared growth of the parental (Δ*ku80*), mutant (Δ*vp1*), and complemented (Δ*vp1-cm*) clones in parallel plaque assays (Fig. 2A). Plaque sizes appear similar between the three strains although a lower number of plaques were consistently observed with the Δ*vp1* mutants. For a more accurate readout we switched to a plaquing efficiency protocol as described (Francia *et al*., 2011), in which there is only a 30 min contact interval between parasite and host. Under these conditions, clear differences were observed in the number of plaques formed between Δ*vp1* mutants and the parental cell line (Fig. 2B). The complementation of the gene in Δ*vp1-cm* restored their normal capacity to form plaques (Fig. 2B). These results suggested that once they invade mutant parasites are able to replicate normally and that the reduction in number of plaques could be due to reduced invasion. To test the ability of these clones to invade host cells, we used a red/green invasion assay where external, attached parasites were stained red while internal, penetrated parasites were stained green (Kafsack *et al*., 2004). Ablation of *TgVP1* caused a 33 ± 4.2% reduction in attachment and a 70 ± 7.4% reduction in invasion, while the complemented clone had values similar to the parent clone (Fig. 2C, n = 3). Interestingly no significant difference in gliding motility based on trail deposition was found between Δ*vp1* parasites and the parental strain Δ*ku80* and Δ*vp1-cm* (Fig. S1).

Δvp1 tachyzoites are defective in microneme secretion

Parasite attachment and invasion is associated with the release of adhesins from micronemes (Carruthers *et al*., 1999). Hence, we examined the role of TgVP1 in release of the micronemal proteins MIC2 and MIC3 (Fig. 3). We

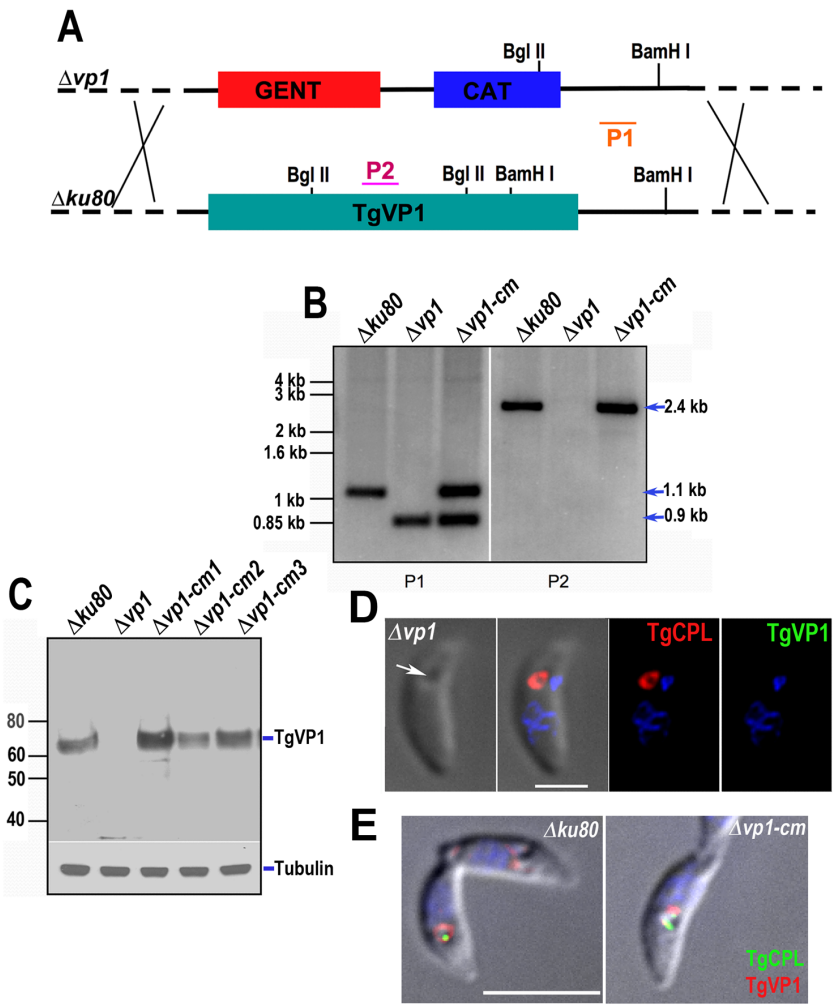

Fig. 1. Targeted disruption and complementation of the *TgVP1* gene.
A. Schematic representation of homologous recombination event in the *T. gondii* genome for cosmid-based gene disruption. The modified cosmid was transfected into *T. gondii* tachyzoites (Δ*ku80*) following standard procedures and one clone (Δ*vp1*) was selected for further analysis. P1 and P2 indicate probes used for the Southern blot analysis in (B).
B. Southern blot analysis of genomic DNA isolated from tachyzoites of Δ*ku80*, Δ*vp1* and Δ*vp1-cm* clones and digested with BamHI and BglII. Probe P1 hybridizes to the 3′ non-coding region present in both loci. P2 hybridizes to a *TgVP1* intron only present in the Δ*ku80* and Δ*vp1-cm* clones.
C. Western blot analysis of total tachyzoite lysates using a Guinea pig anti-TgVP1 antibody (1:500). Mouse anti-α-tubulin (1:1000) was used as loading control.
D. IFA analysis of the Δ*vp1* clone using mouse anti-CPL (1:1000) and Guinea pig anti-TgVP1 (1:100). Secondary antibodies were goat anti-guinea pig (1:1000) and goat anti-mouse (1:1000). The white arrow shows the PLV localization. The PLV is labelled with anti-CPL (red) but shows no signal when using anti-TgVP1 (green) antibody. Scale bar: 2 μm.
E. IFA analysis of the Δ*ku80* and Δ*vp1-cm* strains with mouse anti-CPL (1:200) and rabbit anti-TgVP1 (1:4000). The PLV is labelled with anti-CPL (green) and anti-TgVP1 (red). Scale bar: 5 μm

examined the release of these proteins into the excreted/secreted antigen (ESA) fraction collected from supernatants of extracellular parasites without stimulation (ESA-Const.) or after induction of secretion by ethanol (ESA-Ind.) Δ*vp1* parasites were not able to secrete micronemes constitutively (ESA-Const.) and they responded poorly to stimulation by ethanol (ESA-Ind.) (Fig. 3A). However, the amount of total microneme proteins in the Δ*vp1* parasite lysate was similar to the parental and complemented strains. Figure 3B and C shows the quantification of three independent experiments using the constitutively secreted GRA1 protein as control.

Δvp1 tachyzoites have a maturation defect for CPL but not microneme proteins in the presence of bafilomycin A_1

We reported previously that the parasite cathepsin L (CPL) occupies a compartment that also labels with TgVP1 in extracellular parasites, and that this protease mediates the proteolytic maturation of two proproteins (proM2AP and proMIC3) targeted to micronemes (Parussini *et al.*, 2010). Since this proteolytic maturation is pH-dependent (requires acidic conditions), we next asked whether Δ*vp1* tachyzoites would show differences in maturation of proM2AP, proMIC3, and proMIC5 as compared with those of the parental and complemented clones. Figure S2 shows that there were no significant differences in the maturation of these proteins under normal conditions.

The PLV has two proton pumps, a multisubunit vacuolar H^+-ATPase (TgVATPase), and TgVP1 (Miranda *et al.*, 2010). We reasoned that these two proton pumps could have overlapping functions. To test this, we monitored the maturation of M2AP in the absence or presence of bafilomycin A_1, which is a specific inhibitor of the V-H^+-ATPase when used at very low concentrations (Bowman *et al.*, 1988). Figure S3A and B shows that bafilomycin A_1 had a concentration-dependent inhibitory effect on maturation of proM2AP that was independent of TgVP1 expression. This suggests that TgVATPase, but not TgVP1, contributes to

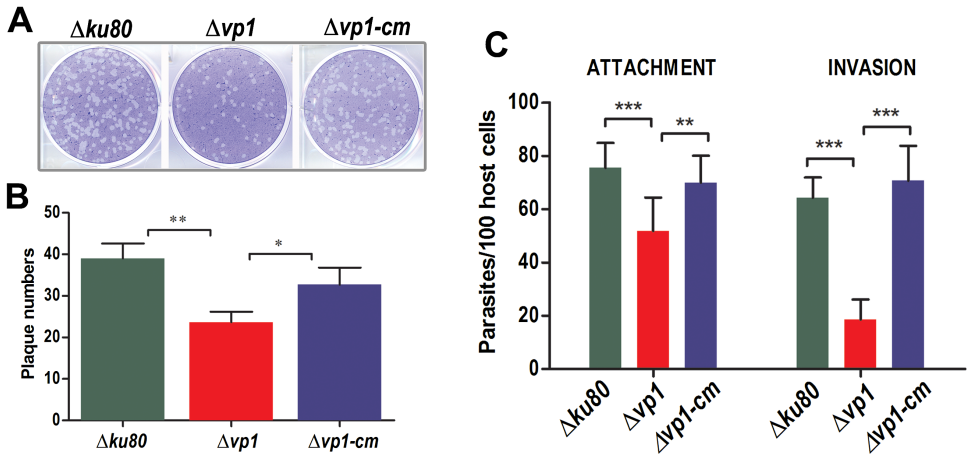

Fig. 2. TgVP1 is required for attachment, and invasion of tachyzoites.
A. Plaque assays comparing growth of tachyzoites of the mutant (Δ*vp1*), parental (Δ*ku80*) and complemented (Δ*vp1-cm*) clones. Each well was infected with 200 parasites and plaques were stained 9 days later.
B. Plaquing efficiency protocol described in more detail in *Experimental procedures*. Data compiled from three independent plaquing efficiency experiments.
C. Red-green assay for quantification of attachment and invasion of *T. gondii* to hTERT cells. Data were compiled from three independent experiments, each one by triplicate, counting eight fields per clone. Fields were randomly selected following the same pattern for all samples. Error bars in (B) and (C) are SD. Data were analysed by GraphPad Prism 5. To compare two groups of data we used one-way ANOVA test.
$^{*}P < 0.05$; $^{**}P < 0.01$; $^{***}P < 0.001$.

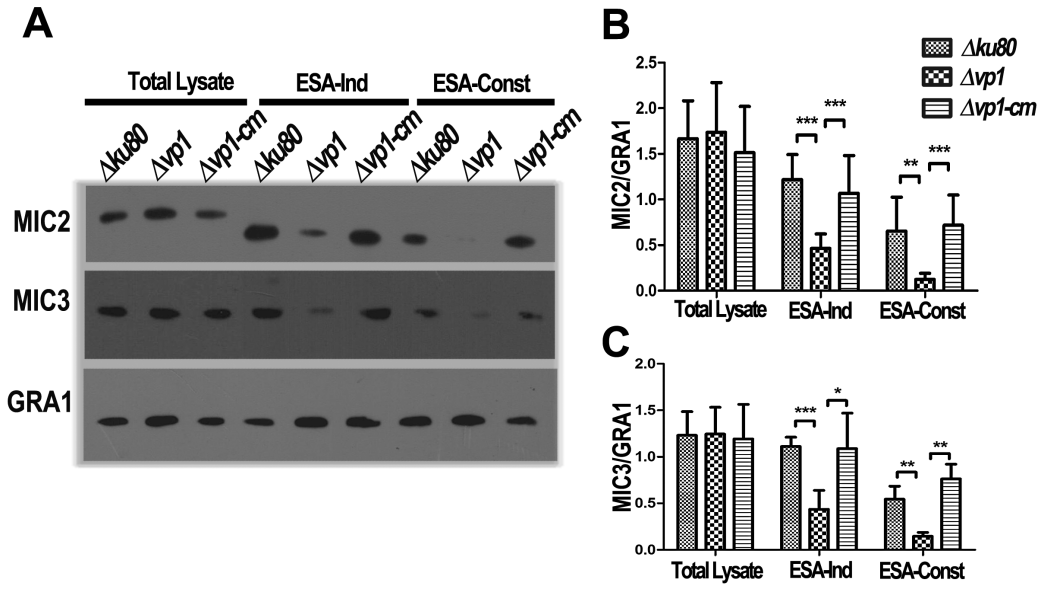

Fig. 3. Δ*vp1* parasites are defective in microneme secretion.
A. Tachyzoites were incubated at 37°C with 1% ethanol (ESA-ind) or in the presence of Invasion Media alone (ESA-Const). Aliquots of the supernatants were analysed by Western blot with an anti-MIC2 antibody (upper panel) or anti-MIC3 antibody (middle panel). The membranes were stripped and reprobed with antibodies against GRA1 for secretion control (lower panel).
B. Quantification of MIC2 secretion by Image J (ratio of MIC2/GRA1). Data were compiled from three independent experiments. Error bars are SD.
C. Quantification of MIC3 secretion. Experiments were standardized to secretion control (GRA1) and quantified using Image J (NIH). Data are pooled from three independent experiments.
To compare two groups of data we used one-way ANOVA test. $^{*}P < 0.05$; $^{**}P < 0.01$; $^{***}P < 0.001$.

the acidification of the compartment(s) where proM2AP undergoes maturation. We next investigated the maturation of proCPL (Fig. 4). In the absence of bafilomycin A_1, proCPL maturation was normal regardless of TgVP1 status (DMSO, Fig. 4A and B) indicating that TgVP1 expression is not required for proCPL maturation when TgVATPase is functional. However, bafilomycin A_1 inhibition of TgVATPase activity caused a delay in proCPL maturation exclusively in Δ*vp1* tachyzoites (Fig. 4C). These findings imply that the proton pumping activities of either TgVATPase or TgVP1 is sufficient for maturation of CPL, indicating a redundancy of function. We also wanted to investigate if the compensatory effect of the TgVATPase would be evident in the lytic cycle of the parasite and for this we used a plaquing efficiency protocol to test whether pre-incubation with bafilomycin A_1 affected tachyzoites of the Δ*vp1* clone to a greater extent. Whereas the low concentration of bafilomycin A_1 barely affected plaque formation by the parental or complemented strain, Δ*vp1* tachyzoites were substantially more sensitive to bafilomycin (Fig. 4D and E). Collectively, these findings indicate independent and overlapping functions for TgVATPase and TgVP1.

Δvp1 tachyzoites show a different pattern of microneme organization

Considering that the Δ*vp1* cells have a microneme secretion defect but their maturation appeared to be normal, we considered the possibility of a defect in the trafficking or biogenesis of micronemes. Figure 5 shows an IFA analysis with anti-MIC2 and anti-M2AP of Δ*vp1* mutants compared with parental (Δ*ku80*) and complemented (Δ*vp1-cm*) strains. We observed that MIC2 and M2AP localize to vesicles and they appear to concentrate around a large vacuole (Fig. 5B, arrowheads). The difference was quite evident when comparing with the pronounced apical localization of micronemes in the Δ*ku80 and* Δ*vp1-cm* strains. Approximately 27% of the Δ*vp1* parasites showed labelling of MIC2 around a large vacuole. This was markedly different from Δ*ku80,* which showed this pattern in only 7% of the cells.

Ca^{2+} and pH homeostasis

Ca^{2+} homeostasis was studied in these mutants by examining store content with thapsigargin (endoplasmic reticulum store), nigericin (acidic stores), ionomycin (all neutral stores) and glycyl-phenylalanine 2-naphthylamide (GPN) (lysosomal stores) (Haller *et al*., 1996; Christensen *et al*., 2002; Lloyd-Evans *et al*., 2008). We did not find a significant difference in the amount of Ca^{2+} released by these ionophores/inhibitors. We found that the cytosolic Ca^{2+} levels of Δ*vp1* parasites are elevated compared to the parental and complemented strains (Table S1). We attribute this difference to the cells being stressed. That acidic pools show a similar amount of Ca^{2+} could be because of the compensatory function of the V-H^+-ATPase.

We also measured intracellular pH of mutant parasites and found no significant difference with pH_i of control strains (data not shown).

Extracellular Δvp1 tachyzoites are more sensitive to environmental stress

We reported previously (Miranda *et al*., 2010) that extracellular tachyzoites overexpressing *TgVP1* were more resistant to salt stress than tachyzoites from the parent strain, suggesting this pump plays a role in the response of the parasite to environmental stress. We therefore investigated whether extracellular Δ*vp1* tachyzoites were more sensitive to environmental stress. We used a plaquing efficiency protocol and counted the number of plaques formed after 4 days of growth of mutant, parental and complemented parasites pre-incubated in an extracellular buffer for 1–6 h. We observed that the number of plaques was significantly lower for the Δ*vp1* parasites after being exposed to extracellular ionic conditions for extended lengths of time (Fig. 6A). This difference is more evident when calculating the ratio of invasion (IR) between Δ*vp1* and Δ*ku80* (Fig. 6B, red columns), which decreases significantly with the time that parasites are left in extracellular buffer. The same IR between Δ*vp1-cm* and Δ*ku80* shows very little change (Fig. 6B, blue columns).

The H^+-PPase protects plant cells from both salt and osmotic stress (Park *et al*., 2005; Lv *et al*., 2008). It is also known that all cells need to regulate their volume continuously (Lang, 2007) so we tested whether tachyzoites of the Δ*vp1* clone would be more sensitive to osmotic stress. We developed a light-scattering protocol to measure volume recovery, the results of which are highlighted in Fig. 6C. This assay was able to demonstrate that changes in osmotic concentration, independent of ion concentration (i.e. absence of salt stress), resulted in regulatory volume changes in the parasites. Tachyzoites were challenged to increasing hypo-osmotic conditions in 5% intervals while continuously observing their regulatory volume capacity. Tachyzoites were observed to regulate their volume but only within a very narrow range of osmolarity. Parental cell lines initially swelled under these conditions and then partially recovered their volume, as measured by light scattering. Under similar stress conditions, Δ*vp1* tachyzoites swelled continuously without recovering. Complemented control tachyzoites had an intermediate response in which swelling was observed but not to the degree seen in the Δ*vp1* tachyzoites (Fig. 6C).

We also investigated the response of tachyzoites to hyperosmotic stress. It has been shown that mutant parasites deficient in the vacuolar type Na^+/H^+ exchanger

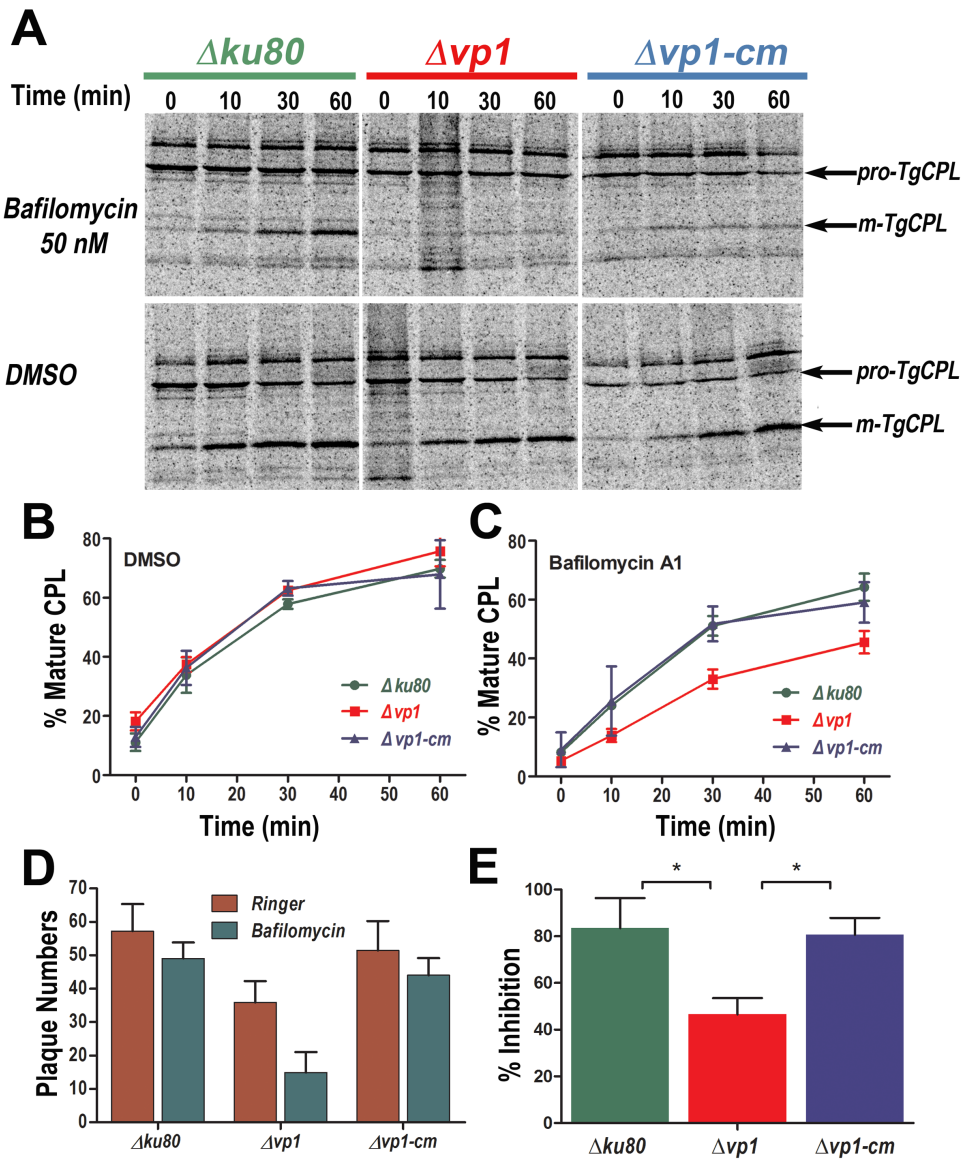

Fig. 4. Δ*vp1* tachyzoites have a TgCPL maturation defect in the presence of bafilomycin A_1.
A. Tachyzoites were pre-incubated for 15 min with 50 nM bafilomycin A_1 or DMSO as control. Metabolically pulse-labelled tachyzoites from Δ*ku80*, Δ*vp1* and Δ*vp1-cm* clones were either kept on ice (0 min) or chased with medium containing unlabelled Met/Cys for the indicated times (10, 30 or 60 min). CPL proteins were immunoprecipitated and analysed by SDS-PAGE and autoradiography. Arrows indicate positions of the immature (pro-TgCPL) and mature (m-TgCPL) forms of CPL. Tachyzoites of the Δ*vp1* clone show impaired maturation of pro-TgCPL after blocking TgVATPase with bafilomycin A_1.
B and C. Quantification of TgCPL maturation in tachyzoites from Δ*ku80*, Δ*vp1* and Δ*vp1-cm* clones for each chase time point in the absence (B, DMSO) or presence (C) of 50 nM bafilomycin A_1. Values are mean ± SD. Data shown are the combined results of three independent experiments.
D. Plaque numbers after pre-incubation of tachyzoites from Δ*ku80*, Δ*vp1* and Δ*vp1-cm* clones in Ringer buffer contain 50 nM bafilomycin A_1. The effect of bafilomycin A_1 was more severe in tachyzoites from the Δ*vp1* clone.
E. Percentage of plaques as compared with controls without bafilomycin A_1 considered as 100%, after incubation of tachyzoites of the different clones in Ringer buffer. Tachyzoites from all clones produced ~ 20% less plaques after incubation with bafilomycin A_1 but tachyzoites from the Δ*vp1* clone produced ~ 55% less plaques than tachyzoites from Δ*ku80* and Δ*vp1-cm* clones. Data are the combined results of three independent experiments.
Data were analysed by GraphPad Prism 5. To compare two groups of data we used one-way ANOVA test. $^*P < 0.05$.

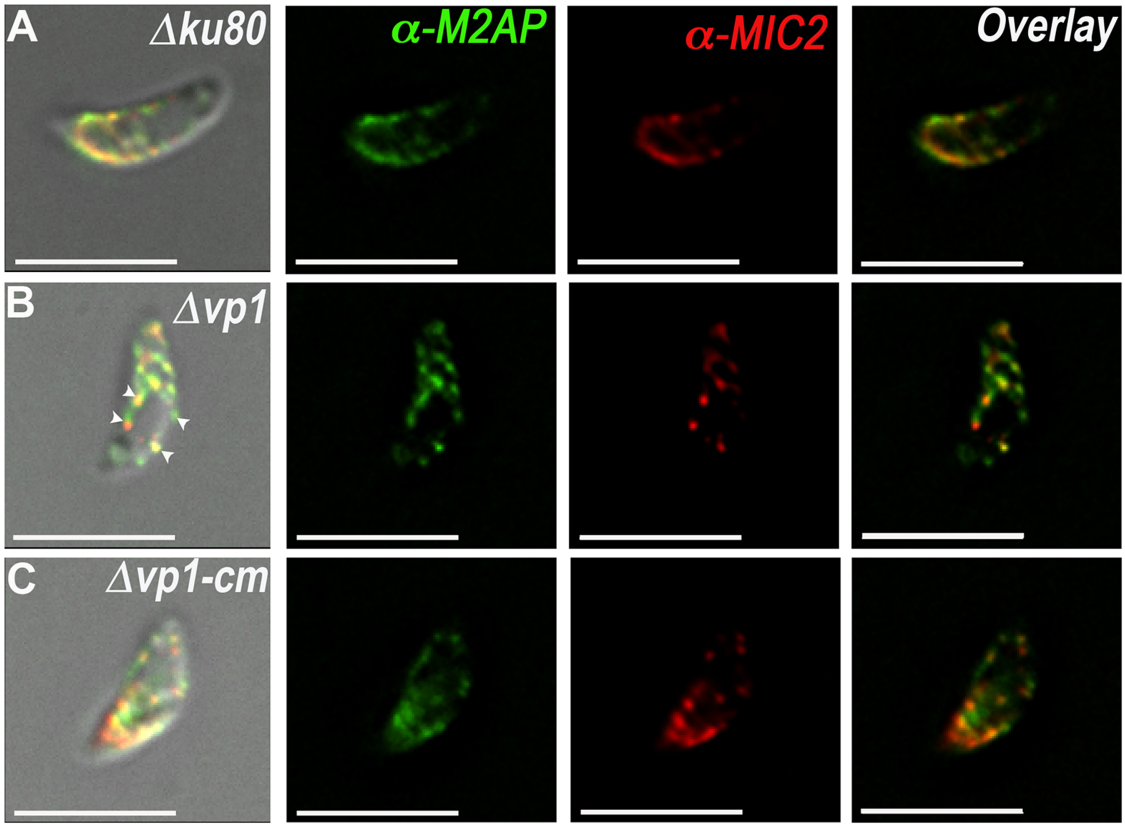

Fig. 5. Extracellular Δ*vp1* show an abnormal distribution of MIC2 and M2AP labelling.
A. IFA analysis of Δ*ku80* parasites with microneme markers MIC2 (1:500) and M2AP (1:500). Normal apical distribution for both proteins is observed. A total of 318 parasites were counted from three independent experiments.
B. IFA analysis of Δ*vp1* parasites showing vesicles labelled with MIC2 and M2AP (arrowheads) surrounding a vacuole. 26.7% of Δ*vp1* parasites show this striking phenotype compared to 7.3% of the Δ*ku80* cells. A total of 299 Δ*vp1* parasites were counted from three different preparations.
C. IFA analysis of Δ*vp1-cm* parasites for MIC2 and M2AP. 263 parasites were counted.
Δ*ku80* and Δ*vp1*, $P = 0.0001$; Δ*ku80* and Δ*vp1-cm*, $P = 0.005$; Δ*vp1* and Δ*vp1-cm*, $P = 0.006$.

(TgNHE3), which localizes to the PLV, are more sensitive to hyperosmotic stress and toxic levels of sodium (Francia *et al*., 2011). In addition, it is known that some organs that are infected by *T. gondii* (liver, spleen, lymphoid tissues) have higher osmolarity than serum (330 versus 300 mOsm) (Go *et al*., 2004) and therefore the ability to tolerate changes in osmolarity would be important for successful infection. To test this response we exposed parasites to a hyper-osmotic buffer for 30 min and then allowed them to form plaques using a plaquing efficiency protocol. Pre-incubation in hyperosmotic conditions (~ 700 mOsm) for 30 min affected all cell lines (parental, Δ*vp1* and complemented) but the effect was more pronounced on the Δ*vp1* parasites (Fig. 6D). The invasion ratio of Δ*vp1*/Δ*ku80* compared with the same ratio of Δ*vp1-cm*/Δ*ku80* highlights this difference (Fig. 6E, compare red and blue columns). In summary, these results indicate that TgVP1 is a critical regulatory element for both the maintenance of salt balance and osmolyte/volume homeostasis.

Knockout of TgVP1 reduces the virulence of tachyzoites

As our results showed that Δ*vp1* tachyzoites were more sensitive to environmental stress we tested their ability to infect mice. We infected mice intraperitoneally (i.p.) with 10 (Fig. 7A) or 50 (Fig. 7B) tachyzoites of the Δ*vp1,* parent, and complemented clones. We observed a 1- to 2-day difference in survival time between mice infected with Δ*vp1* versus those infected with parent or complemented clones. This modest difference is probably due to the hyper-virulent nature of the *Toxoplasma* RH strain masking subtle differences in virulence. Taking into account that dissemination through the circulation is important during natural infection and that this transit exposes tachyzoites to stressful conditions we decided to test the intravenous route (i.v.)

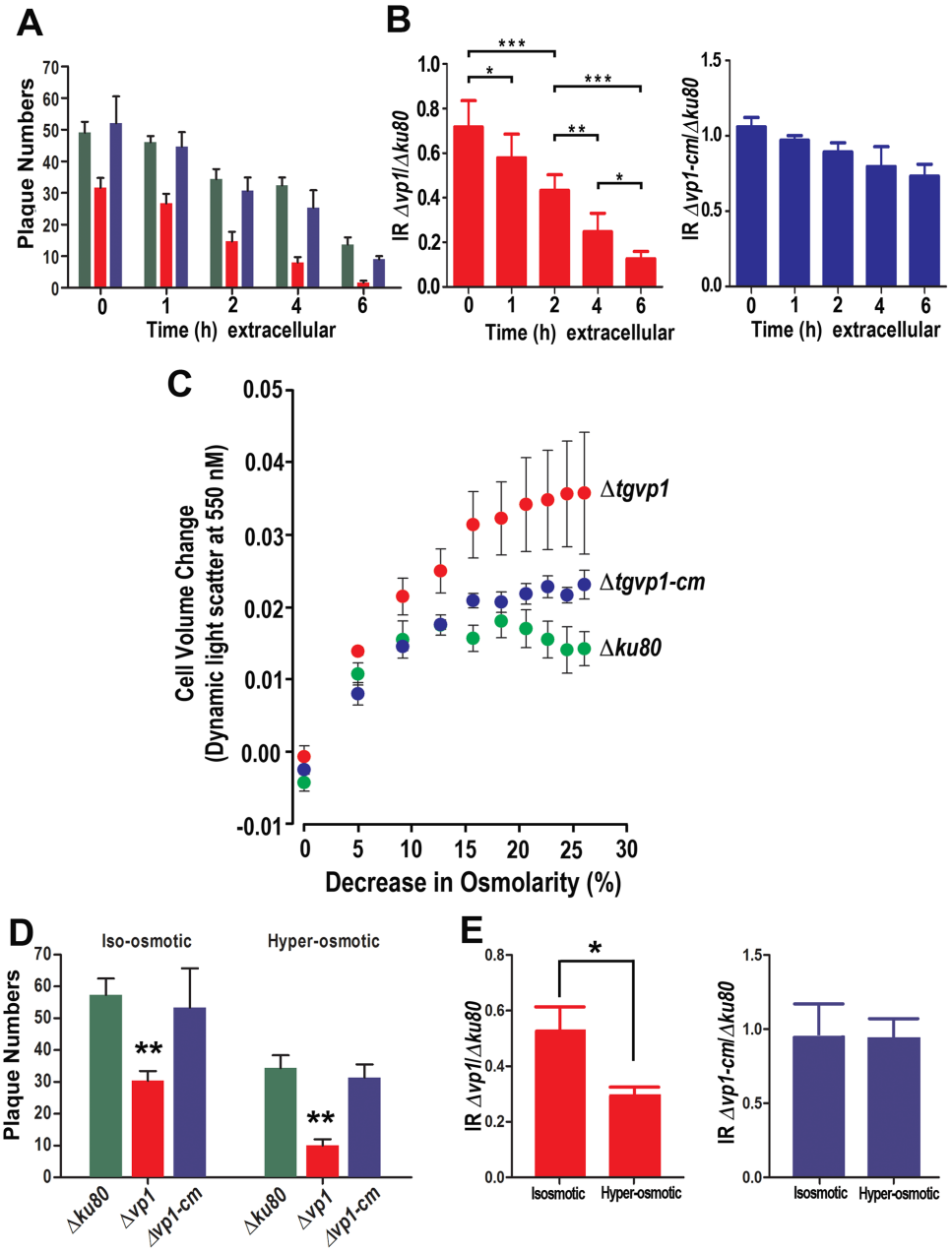

Fig. 6. Extracellular Δ*vp1* parasites are more sensitive to environmental stress.
A. Plaque numbers after pre-incubation of parasites in Ringer buffer for different lengths of time (0, 1, 2, 4 or 6 h). Δ*ku80*, green; Δ*vp1*, red; Δ*vp1-cm*, blue.
B. Ratio (Invasion Ratio, IR) between the number of plaques formed by Δ*vp1* and Δ*ku80* after pre-incubation in an extracellular buffer for 0, 1, 2, 4 and 6 h (red columns). Blue columns show the same ratio calculation for Δ*vp1-cm* and Δ*ku80*. All strains show decreased number of plaques after long extracellular incubation but the decrease in the number of plaques formed by tachyzoites from Δ*vp1* clone was more dramatic than that formed by tachyzoites of Δ*ku80* and Δ*vp1-cm* clones.
C. Effect of hyposmotic conditions on volume changes of tachyzoites from different clones as determined by light scattering. Data are the combined results of three independent experiments.
D. Plaque numbers after pre-incubation of parasites under isosmotic or hyperosmotic conditions.
E. Ratio (IR) of the number of plaques formed by Δ*vp1* and Δ*ku80* submitted to hyperosmotic stress compared to the same ratio for parasites incubated for the same length of time in an isosmotic buffer (red columns). The blue columns show the same calculation between the number of plaques formed by the Δ*vp1-cm* and Δ*ku80* tachyzoites. Tachyzoites from Δ*vp1* clone were less resistant to this treatment than tachyzoites from Δ*ku80* and Δ*vp1-cm* clones and this is evident in the lower ratio obtained under hyperosmotic conditions.
Data from (A,B) and (D,E) were analysed by GraphPad Prism 5. To compare two groups of data we used one-way ANOVA test. $^{*}P < 0.05$; $^{**}P < 0.01$; $^{***}P < 0.001$.

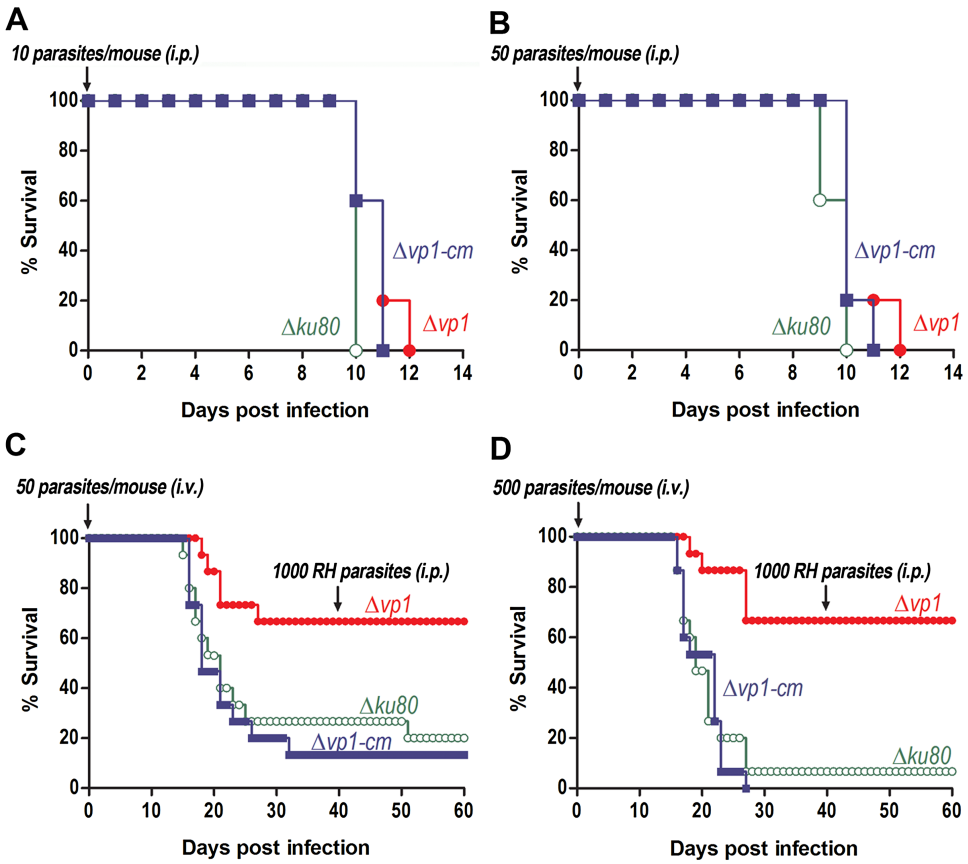

Fig. 7. Knockout of *TgVP1* reduces the virulence of tachyzoites in mice. Ten (A) or 50 (B) tachyzoites were injected intraperitoneally (i.p.) into groups of five female Swiss Webster mice. Fifty (C) or 500 (D) tachyzoites were injected intravenously (i.v.) into groups of five female Swiss Webster mice. All surviving mice were tested 40 days p.i. by Western blot by probing mouse serum against RH lysate (not shown). All mice that survived infection were seropositive. Challenge was done with 1000 tachyzoites of the RH strain. Data are pooled from three independent experiments (at least 15 mice per group). Statistical analysis was performed following the Log-rank/Mantel-Cox method. For i.v. infection with 50 parasites (C) $P = 0.0102$; for infection with 500 parasites (D) $P = 0.0003$. For i.p. infection with 10 parasites (A) $P = 0.4221$; i.p. infection with 50 parasites $P = 0.5118$.

to infect mice. We found that 66.7% of mice infected i.v. with 50 or 500 tachyzoites of the Δ*vp1* clones (Fig. 7C and D) survived past 40 days post infection (p.i.) while only 20% or 6.7% of mice infected with 50 or 500 (respectively) of the Δ*ku80* parasites survived. Mice infected with 50 or 500 Δ*vp1-cm* parasites had a similar survival rate to the parent-infected ones (13.3% and 0%) (Fig. 7C and D). Serum from all surviving mice was analysed 40 days p.i. for the presence of anti-Toxoplasma antibodies and all were seropositive, indicating a successful infection (data not shown). Mice that had been infected with Δ*vp1* parasites, survived an i.p. inoculation with 1000 tachyzoites of the RH strain indicating that these mice were protected against a virulent infection. In addition, we monitored weight of living mice (Fig. S4) and we observed that all of them lost weight around 22–24 days p.i., which indicates that they were infected and became ill around that time. All mice recovered a comparable growth rate to the uninfected controls and there were no obvious signs of illness 8–10 days after challenge. In summary, our data indicate that the virulence of the Δ*vp1* tachyzoites is attenuated compared to the parent and complemented strains.

Discussion

We present here the phenotypic analysis of a straight knockout of the *T. gondii H⁺-PPase* gene. Previous studies have reported downregulation of H⁺-PPase by RNAi or isolation of loss-of-function mutants in *Arabidopsis* (Li *et al.*, 2005). Studies of these mutants revealed that the H⁺-PPase is relevant for development of root, shoot, and flowers, and for fertility (Li *et al.*, 2005). Agricultural plants overexpressing H⁺-PPase display salt- and drought-tolerant phenotypes (Gaxiola *et al.*, 2001).

H⁺-PPases are widespread in all domains of life and they are able to use the energy stored in PPi to pump H⁺

across membranes. The main advantage of these pumps is that they are able to function under stress or with low oxygen levels because they do not need ATP (Maeshima, 2000).

We obtained a clonal line of *T. gondii* tachyzoites, which lack the *TgVP1* gene. These parasites show defects in proper attachment, invasion, microneme secretion, processing of CPL, osmoregulation, and *in vivo* infection. A redundant function of the H^+-ATPase protects these mutant parasites, which are still viable *in vitro*.

Defects in attachment and invasion correlated with the deficient secretion of micronemal proteins by extracellular parasites under physiological conditions (constitutive secretion) or after ethanol induction (induced secretion), as these are adhesins required for these processes (Carruthers *et al.*, 1999). However, the deficient secretion of micronemal proteins is not due to a deficit in their processing, as suggested by the experiments with proM2AP, proMIC3 and proMIC5. Rather, we found that the localization of MIC2 and M2AP in mutant parasites is altered and a higher percentage of mutant parasites showed a vesicular distribution preferentially surrounding an area with the appearance of a large vacuole. Our interpretation is that these parasites are defective in the formation of microneme organelles or their trafficking to the apical end of the parasites. Accordingly, these defective micronemes are sub-optimally positioned for secretion, which is predicted to compromise the release of microneme contents, compromising parasite invasion.

Processing of CPL proceeded at a normal rate in the Δ*vp1* tachyzoites compared to tachyzoites of the parental and complemented clones but showed a significant delay when a V-H^+-ATPase inhibitor (bafilomycin A_1) was present, suggesting that CPL maturation occurs in a compartment where both TgVP1 and TgVATPase are present. Although CPL has been proposed to function as a maturase for M2AP (Parussini *et al.*, 2010), processing of M2AP proprotein in the presence of bafilomycin A_1 was not affected in the Δ*vp1* tachyzoites. This could be because CPL maturation is not completely blocked by bafilomycin A_1 in Δ*vp1* tachyzoite or because CPL is not the only maturase for M2AP and other maturases might be less dependent upon TgVP1 acidification in the absence of V-H^+-ATPase activity. Another explanation could be that the pulse-chase experiments only detect nascent CPL and an existing pool of mature CPL exists in the parasites prior to bafilomycin A_1 treatment and this pool is presumably available to catalyse M2AP maturation even when nascent CPL maturation is impaired.

Micronemes are discharged in response to the elevation of parasite intracellular Ca^{2+} caused naturally by exposure to extracellular conditions or artificially by conditions that elevate intracellular Ca^{2+} (Carruthers *et al.*, 1999). Interestingly, mutant tachyzoites lacking TgA1, the acidocalcisome Ca^{2+}-ATPase, also show deficient microneme secretion in the presence of ionophores, as compared to control tachyzoites, as well as defects in attachment and invasion (Luo *et al.*, 2001; 2005). We have shown previously that the PLV as well as acidocalcisomes contains Ca^{2+} (Rohloff *et al.*, 2011) so it is possible that these acidic calcium stores (Patel and Docampo, 2010) are involved in the intracellular Ca^{2+} increase needed for microneme secretion. Our hypothesis is that the PLV plays a major role in regulating cytoplasmic Ca^{2+} fluctuations and the acidic environment of the compartment would contribute to its Ca^{2+} uptake ability. Both TgVP1 and TgVATPase could contribute to this activity. We did not find differences in the amount of Ca^{2+} released by either nigericin (acidic compartment) or GPN (lysosomal compartment) indicating that the free stored Ca^{2+} in the PLV has not changed in the Δ*vp1* mutants. However, the cytosolic Ca^{2+} levels are elevated in the Δ*vp1* mutants, which could be the result of a leaky PLV. We also did not find that the endoplasmic reticulum Ca^{2+} content (tested with thapsigargin) was changed. Another possible explanation of a higher cytosolic Ca^{2+} would be that these mutant cells are more sensitive to the stress they have to be exposed to during loading with Fura-2 AM leading to higher cytosolic Ca^{2+}. Higher cytosolic Ca^{2+} has also been observed in other mutants (TgA1 and TgNHE3) associated with a microneme secretion defect (Luo *et al.*, 2005; Francia *et al.*, 2011).

The ability to control cell volume is critical for cell function (Hoffmann *et al.*, 2009). Most cells have the capacity to counteract volume perturbations by the process of Regulatory Volume Decrease (RVD) or Regulatory Volume Increase (RVI) (Hoffmann *et al.*, 2009). When cell volume is disturbed, different signalling events could be triggered by swelling as well as shrinkage, which could play a role in the cell volume regulatory response (Pedersen *et al.*, 2001). The plant vacuole plays in important role in osmoregulation for the plant cell (Barkla and Pantoja, 1996). The organelle acts as a water reservoir for the cytosol and the highly osmosensitive chloroplast. The tonoplast (plant vacuole membrane) is highly permeable to water due to the presence of water channels (Barkla and Pantoja, 1996).

For entering a host cell, *T. gondii* relies on its own motility and on the ability to establish a structure called the moving junction (Besteiro *et al.*, 2011). During the process of entry, the parasite squeezes itself through the moving junction, a process that results in deformations of its cell shape. Our hypothesis is that these changes in the parasite cell shape are accompanied by large relative changes in cell volume. These changes could be accomplished by the interaction of several solute transporters and exchangers that are linked to the proton gradient established by TgVP1 and TgVATPase. The connectivity of these exchange mechanisms with the proton gradient has been established in the

PLV (Miranda *et al.*, 2010; Francia *et al.*, 2011). The phenotypic defects of the Δ*vp1* mutants would be the result of a defective H^+-gradient leading to defective capacity to accumulate osmolytes resulting in a defective cell volume response, which would affect invasion and other stress responses. In this regard, we found that Δ*vp1* parasites are more sensitive to extracellular ionic concentrations, hyper-osmotic or hypo-osmotic stress. This would be especially evident when the parasite is outside, surrounded by a variable osmotic environment and/or for performing a function requiring cell volume changes like invasion. We found that the action of the V-H^+-ATPase partially rescues the defects due to lack of TgVP1. The results from this study further implicate the involvement of TgVP1 as both a mechanism for sodium regulation (Miranda *et al.*, 2010) and a participant in osmotic/volume regulatory mechanisms. We found a significantly stronger defect in invasion in the Δ*vp1* mutants when allowed to invade after a pre-treatment with the specific V-H^+-ATPase inhibitor, bafilomycin A_1. Very low concentrations of the inhibitor were used so it would not affect the normal invasion of parental parasites.

We also tested the levels of PP_i because it was previously shown in *Arabidopsis* that the H^+-PPase functions in hydrolysis of PP_i and mutants for the enzyme accumulate the substrate during early seedling (Ferjani *et al.*, 2012). We have shown previously that PP_i has a regulatory role on glycolysis and an increase in its concentrations could explain some of the observed phenotypes. We did not detect a significant difference in PP_i levels in the Δ*vp1* mutants (data not shown), which are probably controlled by the soluble pyrophosphatase (Pace *et al.*, 2011).

In summary, defects in microneme secretion, attachment, invasion, processing of some proteins and osmotic fragility made Δ*vp1* tachyzoites less able to grow *in vitro* and *in vivo* indicating that TgVP1 fulfils an important role in the *T. gondii* lytic cycle. The parasite is exposed to dramatic ionic changes upon egress while it actively needs to invade host cells to continue with its lytic cycle. We think that the PLV plays a central role during the extracellular phase of the parasite not only in resisting environmental stress but also as it prepares itself for invading the next host cell. This would be consistent with what is known about the plant vacuole, which is home to a complex set of functions (storage, sorting, stress, etc.). Likewise, it seems feasible that the PLV is involved in a complex set of functions, especially significant during the extracellular phase of *T. gondii,* and analysing mutants like Δ*vp1* will contribute to the elucidation of its role in the lytic cycle of the parasite. Our studies demonstrate that *T. gondii* tachyzoites can undergo a regulatory volume decrease after hypo-osmotic stress underscoring the role of osmoregulation during invasion.

Experimental procedures

Parasite cultures and generation of mutant strains

Toxoplasma gondii tachyzoites were grown in hTERT human fibroblasts as described before (Moreno and Zhong, 1996). The parental strain used to generate knockouts were Δ*ku80* (Fox *et al.*, 2009), which was transfected with a modified cosmid generated by recombineering as previously described (Brooks *et al.*, 2010). Cosmid PSBM180 was used and the modification cassette was amplified from plasmid pH3CG, including genes for gentamicin (bacterial selection), and chloramphenicol (*T. gondii* selection), flanked by 50 bp of *TgVP1* sequence. The forward primer was

5′-actcgtcgtcttcatctcgtggacacaacagaacgctttcgacttccatcCC TCGACTACGGCTTCCATTGGCAAC-3′, and the reverse primer was 5′-atgaacgtacacaaacagataccaaaaaaaattgtacg cgttcaccctgtATACGACTCACTATAGGGCGAATTGG-3′. The PCR product was introduced by electroporation and cells selected with kanamycin and gentamicin. The modified cosmid was used to disrupt the native loci in Δ*ku80* tachyzoites by double homologous recombination and replacement of the entire coding region, and stable clones were derived by chloramphenicol (20 μM) selection. For complementation analysis, the cosmid PSBM180 (which includes the *TgVP1* genomic locus plus a selectable marker; DHFR-TS) was transfected into Δ*Tgvp1* tachyzoites and the parasites were selected with 1 μM pyrimethamine.

Although we do not know the fate of the construct (episomal or integrated), the findings in Fig. 1 indicate that the construct did not target to the *TgVP*1 locus by double-crossover homologous recombination since the P1 probe shows that the knockout construct remains at the locus. Although it would have been ideal to target the *TgVP1* cosmid to a specific neutral locus, this was not possible due to an inability to insert a specific targeting sequence into the cosmid.

For Southern blot analysis total genomic DNA from Δ*ku80*, Δ*vp1* and Δ*vp1-cm* (1.3 μg per lane) were digested with BamHI and BglII, resolved on 0.7% agarose and transferred to nylon membranes. Blots were hybridized with radiolabelled DNA fragments (P1, 413 bp and P2, 700 bp) of *TgVP1* prepared by randomly primed synthesis with Klenow DNA polymerase and [α-^{32}P]-dCTP. Probe P2 (*TgVP1* intron) hybridizes to native *TgVP1*; probe P1 (3′ non-coding region present in both loci) hybridizes to both. The primers used were, for probe P1: forward, 5′-GCTAGACCACAACGGAAGCA AAC-3′ and reverse, 5′-CGAGCAACGGTAACACTCCTGTA-3′, and for probe P2: forward 5′-TCGTCGTGTTCTCCT CTATCT-3′, and reverse: 5′-GGACCACCTCAATCCAGTCG-3′. Autoradiographs were stripped and reprobed.

Growth assays

Two different protocols were used for plaque assays. For experiments testing growth, plaques of Δ*ku80*, Δ*vp1* and Δ*vp1-cm* parasites (200 parasites per well) were allowed to form in monolayers of hTERT cells for 8–9 days, fixed and stained with crystal violet. Plaquing efficiency was measured infecting hTERT fibroblasts with 1000 parasites per

well and allowing contact with host cells for 30 min. At this point, wells were washed with PBS, fresh media added and parasites allowed to grow for 4 days, fixed and stained with crystal violet. For fitness testing parasites were pre-incubated in Ringer buffer (155 mM NaCl, 3 mM KCl, 1 mM $MgCl_2$, 3 mM NaH_2PO_4-H_2O, 10 mM HEPES, pH 7.2, 10 mM glucose) for the times indicated in the figure. For osmotic stress experiments, parasites were pre-incubated at 37°C for 30 min in either hyperosmotic (64 mM NaCl, 4 mM KCl; 1.8 mM $CaCl_2$, 0.53 mM $MgCl_2$, 5.5 mM Glucose, 10 mM HEPES, pH 7.4, 700 mM mannitol) or isosmotic (~ 300 mOsm) Ringer buffer, and used for infection as for the fitness experiments.

Red/Green invasion assay was performed as described (Kafsack *et al.*, 2004) with some modifications. Briefly, sub-confluent hTERT monolayers grown in 12-well plates were challenged with 1×10^7 tachyzoites, resuspended in Endo buffer (Endo and Yagita, 1990) (44.7 mM K_2SO_4, 10 mM $MgSO_4$, 106 mM sucrose, 5 mM glucose, 20 mM Tris-H_2SO_4, 3.5 mg ml^{-1} BSA, pH 8.2) and allowed to settle for 20 min at 37°C. Next the buffer was replaced with invasion media (DMEM + 10 mM HEPES, pH 7.4, and 3% FBS) and incubated for 2 min at 37°C. Subsequently, wells were washed with PBS and fixed with 2.5% formaldehyde. Blocking was with 10% FBS for 30 min at room temperature and fixed cells were first incubated with rabbit anti-SAG1 polyclonal antibody (1:1000), and next with the anti-SAG1 monoclonal antibody (1:500) following a previous protocol (Kafsack *et al.*, 2004). Counting was performed using an Olympus fluorescence microscope and data were compiled from three independent experiments, each one by triplicate, counting eight fields/clone, selected at random, at 400× total magnification. Statistical analysis was performed using the Student's *t*-test. Differences were considered significant if *P*-values were < 0.05.

Immunofluorescence and Western blot analysis

Indirect immunofluorescence assays (IFA) were performed on freshly collected tachyzoites washed with buffer A with glucose (BAG, 116 mM NaCl, 5.4 mM KCl, 0.8 mM $MgSO_4$, 50 mM HEPES, pH 7.2, and 5.5 mM glucose) and fixed with 4% formaldehyde for 1 h, permeabilized with 0.3% Triton X-100 for 20 min, and blocked with 3% bovine serum albumin (Miranda *et al.*, 2010). Immunofluorescence was performed as previously described (Miranda *et al.*, 2010) and primary and secondary antibodies concentrations are indicated in the figure legends. Fluorescence images were collected with an Olympus IX-71 inverted fluorescence microscope with a Photometrix CoolSnapHQ CCD camera driven by DeltaVision software (Applied Precision, Seattle, WA). Collected images were deconvolved using Softworx deconvolution software (Applied Precision, Seattle, WA). For all images, 15 cycles of enhanced ratio deconvolution were used.

Western blot analysis was performed as previously described (Miranda *et al.*, 2010). We used the anti-TgVP1 polyclonal antibody at a dilution of 1:500 and secondary goat anti-Guinea pig antibody conjugated with HRP at 1:5000. Mouse anti-α-tubulin at a dilution of 1:1000 was used as a loading control.

Gliding motility

Glass chamber slides were coated overnight at 4°C with 50% fetal bovine serum in PBS (pH 7.4) and slides washed with PBS (Wetzel *et al.*, 2004). Freshly lysed parasites, washed and suspended in HHE (Hank's Balanced Salt, 10 mM HEPES, 1 mM EGTA) were allowed to glide on FBS coated slides, at 37°C for 15 min. Fixation was with 4% paraformaldehyde and staining was performed with Rabbit anti-SAG1 antibody 1:1000 directly conjugated to Alexa 488 fluorochrome 1:1000. A trail was considered circular if the diameter was 11 μm or less; trails that were larger in diameter or straight were counted as non-circular. Approximately 100 trails were enumerated per strain in each experiment. Although Δ*vp1* show a small decrease in circular trails when compared to Δ*ku80* and Δ*vp1-cm*, we did not find a significant difference among the three strains. Values are mean ± SD. Data are the combined results of three independent experiments and analysed by GraphPad Prism 5.

Microneme secretion

The secretion of micronemes by tachyzoites of the Δ*ku80,* Δ*vp1*, and Δ*vp1-cm1* clones were measured as described (Carruthers *et al.*, 1999). Tachyzoites were harvested and washed twice in invasion medium (IM) (DMEM plus 20 mM HEPES), and resuspended in IM at 4×10^8 cells per ml. Excretion/secretion antigen (ESA) fraction was obtained by collecting the supernatant of parasites incubated for 30 min in a 37°C water bath (ESA-Const.). The stimulated secretion of micronemes was obtained by incubating parasites for 2 min in IM containing 1% ethanol. Secretion was stopped by placing the tubes on ice. Cells were removed by centrifugation at 1000 *g* for 10 min at 4°C. Proteins in the supernatants were separated by SDS-PAGE, and used for Western blot analysis. Mouse anti-MIC2 serum was used at a dilution of 1:8000, and secondary Goat anti-mouse HRP-conjugated antibody. Rabbit anti-MIC3 was used at 1:500. Mouse anti-GRA1 at 1:1000 was used as secretion control. Quantification was done using ImageJ (NIH). Data are pooled from three independent experiments.

Metabolic labelling and immunoprecipitation

Immunoprecipitation was performed as described before (Parussini *et al.*, 2010). Freshly lysed tachyzoites were harvested and resuspended in Met/Cys-free DMEM containing 10 mM HEPES, pH 7.0, and 2 mM L-Gln. Parasites were pre-incubated for 15 min, at room temperature with solvent control (DMSO) or bafilomycin A_1, then pulsed-labelled with 300 μCi [^{35}S] Met/Cys (Perkin Elmer) for 10 min, at 37°C, chased in unlabelled medium with 5 mM methionine, 5 mM cysteine and bafilomycin A_1 for the indicated times. Parasites were washed with medium, resuspended in 0.8 ml RIPA buffer (50 mM Tris, pH 7.5, 100 mM NaCl, 5 mM EDTA, pH 8.0, 1% Triton X-100, 0.5% sodium deoxycholate, 0.2% SDS, 10 mg ml^{-1} RNase A, 20 μg ml^{-1} DNase I, and protease inhibitors), incubated 30 min at 0°C, and insoluble material was removed by centrifugation (13 000 r.p.m., 10 min, at 4°C). Antibodies to CPL, MIC3, MIC5, or M2AP were incubated with 400 μl of extract for 1 h, at 4°C, followed by

addition of 100 µl 10% (v/v) slurry of protein G-sepharose beads, and 1 h incubation at 4°C, with gentle rocking. Immune complexes were washed four times with 1 ml RIPA buffer before boiling in SDS-PAGE sample buffer containing 2% β-mercaptoethanol, separated by SDS-PAGE, incubated in fluorographic enhancer (Amplify, Amersham), dried in cellophane, and exposed to Storage Phosphor Screen.

Intracellular Ca^{2+} and pH measurements

Parasites were loaded with Fura 2-AM as described (Moreno and Zhong, 1996). After harvesting and purifying the parasites they were washed twice at 500 *g* for 10 min in BAG. Cells were resuspended to a final density of 1×10^9 cells ml^{-1} in loading buffer, which consisted of BAG plus 1.5% sucrose and 5 µM Fura 2-AM. The suspensions were incubated for 25 min in a 26°C water bath with mild agitation. Subsequently, the cells were washed twice and resuspended to a final density of 1×10^9 cells ml^{-1} in the same buffer. A 50 µl aliquot of the cell suspension was diluted into 2.5 ml of Ringer buffer (2×10^7 cells ml^{-1} final density) in a cuvette placed in a Hitachi F-4500 spectrofluorometer. Excitation was at 340 and 380 nm and emission at 510 nm. The Fura 2 response was calibrated from the ratio of 340/380 nm fluorescence values after subtraction of the background fluorescence of the cells at 340 and 380 nm as previously described (Grynkiewicz *et al.*, 1985).

For pH measurements parasites were loaded following a similar procedure but using BCECF-AM (2′,7′-Bis-(2-Carboxyethyl)-5-(and-6)-Carboxyfluorescein, Acetoxymethyl Ester) as intracellular pH indicator. Calibrations were done following published protocols (Moreno *et al.*, 1998).

Cell volume regulation during hypo-osmotic stress

Analysis of cell volume change was based on previous studies in which changes in cell volume were determined by the degree of light scattering at 550 nM (Rohloff *et al.*, 2003). These approaches have worked very well for other unicellular parasites such as trypanosomes (Rohloff *et al.*, 2003). The reagents employed in these experiments were designed to ensure that ionic conditions (for example Na^+ and K^+ concentrations) were held constant during hypo-osmotic treatment. Hypo-osmotic conditions were therefore manipulated through variations in the amount of mannitol in the buffers (de Jesus *et al.*, 2010). Cells were harvested and resuspended in isosmotic buffer (64 mM NaCl, 4.0 mM KCl, 0.5 mM $MgCl_2$, 1.8 mM $CaCl_2$, 5.0 mM HEPES-Na buffer, pH 7.3, 5.5 mM glucose, and 150 mM mannitol; final osmolarity of 282 mOsm). Cells (2 ml initial volume at a final concentration of 3×10^7 cells ml^{-1}) were transferred to a 4 ml cuvette and light scattering at 550 nm continuously monitored during addition of hypo-osmotic buffer (64 mM NaCl, 4.0 mM KCl, 0.5 mM $MgCl_2$, 1.8 mM $CaCl_2$, 5.0 mM HEPES-Na buffer, pH 7.3, 5.5 mM glucose, final osmolarity 132 mOsm). Over the course of 20 min the initial isosmotic conditions were diluted with hypo-osmotic buffer at a rate of 200 µl addition every 2 min (initial osmotic dilution rate at 5%). Light scattering was monitored continuously during this time using a SpectraMax M2c plate reader. Hypo-osmotic dilution experiments resulted in a stepwise decrease in absorption at 550 nm every 2 min. This decrease was due to 2 factors: the dilution of cells that occurs by adding buffer and the change in cell volume that results from the addition of hypo-osmotic buffer. To distinguish between the two phenomena, controls were done in which an equal volume of iso-osmotic buffer was added to control for the contribution of the dilution effect to the light scattering measurements.

In vivo *virulence assay*

Groups of five female Swiss Webster mice 8–9 weeks old were infected intraperitoneally (i.p.) or intravenously (i.v.) (Lagal *et al.*, 2010). Serum from all surviving mice was assayed 40 days post infection by Western blot by probing it against an RH tachyzoite lysate (not shown). Surviving mice were challenged at this time with 1000 RH parasites (i.p. inoculation). Mice were monitored daily over a period of 8 weeks after infection. Data were pooled from three independent experiments. Statistical analysis was performed following the Log-rank/Mantel-Cox method.

Acknowledgements

We thank David Bzik for the Δ*ku80* parasites and Boris Striepen for cosmids, plasmids and advise. Samantha Lie Tjauw provided excellent technical support. This work was supported by NIH Grants AI096836 (to SNJM) and AI063263 (to VBC). DP was partially supported by an NIH T32 training grant AI-60546 to the Center for Tropical and Emerging Global Diseases. JL was partially funded by the Natural Science Foundation of China (No 31302075).

References

Baltscheffsky, H., Von Stedingk, L.V., Heldt, H.W., and Klingenberg, M. (1966) Inorganic pyrophosphate: formation in bacterial photophosphorylation. *Science* **153:** 1120–1122.

Baltscheffsky, M., Schultz, A., and Baltscheffsky, H. (1999) H^+-PPases: a tightly membrane-bound family. *FEBS Lett* **457:** 527–533.

Barkla, B.J., and Pantoja, O. (1996) Physiology of ion transport across the tonoplast of higher plants. *Annu Rev Plant Physiol Plant Mol Biol* **47:** 159–184.

Baykov, A.A., Bakuleva, N.P., and Rea, P.A. (1993) Steady-state kinetics of substrate hydrolysis by vacuolar H^+-pyrophosphatase. A simple three-state model. *Eur J Biochem* **217:** 755–762.

Belogurov, G.A., and Lahti, R. (2002) A lysine substitute for K^+. A460K mutation eliminates K^+ dependence in H^+-pyrophosphatase of *Carboxydothermus hydrogenoformans*. *J Biol Chem* **277:** 49651–49654.

Besteiro, S., Dubremetz, J.F., and Lebrun, M. (2011) The moving junction of apicomplexan parasites: a key structure for invasion. *Cell Microbiol* **13:** 797–805.

Bowman, E.J., Siebers, A., and Altendorf, K. (1988) Bafilomycins: a class of inhibitors of membrane ATPases from microorganisms, animal cells, and plant cells. *Proc Natl Acad Sci USA* **85:** 7972–7976.

Brooks, C.F., Johnsen, H., van Dooren, G.G., Muthalagi, M.,

Lin, S.S., Bohne, W., *et al*. (2010) The toxoplasma apicoplast phosphate translocator links cytosolic and apicoplast metabolism and is essential for parasite survival. *Cell Host Microbe* **7:** 62–73.

Carruthers, V.B., Giddings, O.K., and Sibley, L.D. (1999) Secretion of micronemal proteins is associated with toxoplasma invasion of host cells. *Cell Microbiol* **1:** 225–235.

Christensen, K.A., Myers, J.T., and Swanson, J.A. (2002) pH-dependent regulation of lysosomal calcium in macrophages. *J Cell Sci* **115:** 599–607.

Docampo, R., and Moreno, S.N. (2011) Acidocalcisomes. *Cell Calcium* **50:** 113–119.

Drozdowicz, Y.M., and Rea, P.A. (2001) Vacuolar H^+-pyrophosphatases: from the evolutionary backwaters into the mainstream. *Trends Plant Sci* **6:** 206–211.

Drozdowicz, Y.M., Shaw, M., Nishi, M., Striepen, B., Liwinski, H.A., Roos, D.S., and Rea, P.A. (2003) Isolation and characterization of TgVP1, a type I vacuolar H^+-translocating pyrophosphatase from *Toxoplasma gondii*. The dynamics of its subcellular localization and the cellular effects of a diphosphonate inhibitor. *J Biol Chem* **278:** 1075–1085.

Endo, T., and Yagita, K. (1990) Effect of extracellular ions on motility and cell entry in *Toxoplasma gondii*. *J Protozool* **37:** 133–138.

Ferjani, A., Segami, S., Horiguchi, G., Sakata, A., Maeshima, M., and Tsukaya, H. (2012) Regulation of pyrophosphate levels by H^+-PPase is central for proper resumption of early plant development. *Plant Signal Behav* **7:** 38–42.

Fox, B.A., Ristuccia, J.G., Gigley, J.P., and Bzik, D.J. (2009) Efficient gene replacements in *Toxoplasma gondii* strains deficient for nonhomologous end joining. *Eukaryot Cell* **8:** 520–529.

Francia, M.E., Wicher, S., Pace, D.A., Sullivan, J., Moreno, S.N., and Arrizabalaga, G. (2011) A *Toxoplasma gondii* protein with homology to intracellular type Na^+/H^+ exchangers is important for osmoregulation and invasion. *Exp Cell Res* **317:** 1382–1396.

Garcia-Contreras, R., Celis, H., and Romero, I. (2004) Importance of *Rhodospirillum rubrum* H^+-pyrophosphatase under low-energy conditions. *J Bacteriol* **186:** 6651–6655.

Gaxiola, R.A., Li, J., Undurraga, S., Dang, L.M., Allen, G.J., Alper, S.L., and Fink, G.R. (2001) Drought- and salt-tolerant plants result from overexpression of the AVP1 H^+-pump. *Proc Natl Acad Sci USA* **98:** 11444–11449.

Go, W.Y., Liu, X., Roti, M.A., Liu, F., and Ho, S.N. (2004) NFAT5/TonEBP mutant mice define osmotic stress as a critical feature of the lymphoid microenvironment. *Proc Natl Acad Sci USA* **101:** 10673–10678.

Grynkiewicz, G., Poenie, M., and Tsien, R.Y. (1985) A new generation of Ca^{2+} indicators with greatly improved fluorescence properties. *J Biol Chem* **260:** 3440–3450.

Haller, T., Dietl, P., Deetjen, P., and Volkl, H. (1996) The lysosomal compartment as intracellular calcium store in MDCK cells: a possible involvement in InsP3-mediated Ca^{2+} release. *Cell Calcium* **19:** 157–165.

Hoffmann, E.K., Lambert, I.H., and Pedersen, S.F. (2009) Physiology of cell volume regulation in vertebrates. *Physiol Rev* **89:** 193–277.

Huynh, M.H., and Carruthers, V.B. (2009) Tagging of endogenous genes in a *Toxoplasma gondii* strain lacking Ku80. *Eukaryot Cell* **8:** 530–539.

de Jesus, T.C., Tonelli, R.R., Nardelli, S.C., da Silva Augusto, L., Motta, M.C., Girard-Dias, W., *et al*. (2010) Target of rapamycin (TOR)-like 1 kinase is involved in the control of polyphosphate levels and acidocalcisome maintenance in *Trypanosoma brucei*. *J Biol Chem* **285:** 24131–24140.

Kafsack, B.F., Beckers, C., and Carruthers, V.B. (2004) Synchronous invasion of host cells by *Toxoplasma gondii*. *Mol Biochem Parasitol* **136:** 309–311.

Lagal, V., Binder, E.M., Huynh, M.H., Kafsack, B.F., Harris, P.K., Diez, R., *et al*. (2010) *Toxoplasma gondii* protease TgSUB1 is required for cell surface processing of micronemal adhesive complexes and efficient adhesion of tachyzoites. *Cell Microbiol* **12:** 1792–1808.

Lang, F. (2007) Mechanisms and significance of cell volume regulation. *J Am Coll Nutr* **26:** 613S–623S.

Lemercier, G., Dutoya, S., Luo, S., Ruiz, F.A., Rodrigues, C.O., Baltz, T., *et al*. (2002) A vacuolar-type H^+-pyrophosphatase governs maintenance of functional acidocalcisomes and growth of the insect and mammalian forms of *Trypanosoma brucei*. *J Biol Chem* **277:** 37369–37376.

Li, J., Yang, H., Peer, W.A., Richter, G., Blakeslee, J., Bandyopadhyay, A., *et al*. (2005) Arabidopsis H^+-PPase AVP1 regulates auxin-mediated organ development. *Science* **310:** 121–125.

Lin, S.M., Tsai, J.Y., Hsiao, C.D., Huang, Y.T., Chiu, C.L., Liu, M.H., *et al*. (2012) Crystal structure of a membrane-embedded H^+-translocating pyrophosphatase. *Nature* **484:** 399–403.

Lloyd-Evans, E., Morgan, A.J., He, X., Smith, D.A., Elliot-Smith, E., Sillence, D.J., *et al*. (2008) Niemann-Pick disease type C1 is a sphingosine storage disease that causes deregulation of lysosomal calcium. *Nat Med* **14:** 1247–1255.

Lopez-Marques, R.L., Perez-Castineira, J.R., Losada, M., and Serrano, A. (2004) Differential regulation of soluble and membrane-bound inorganic pyrophosphatases in the photosynthetic bacterium *Rhodospirillum rubrum* provides insights into pyrophosphate-based stress bioenergetics. *J Bacteriol* **186:** 5418–5426.

Luo, S., Vieira, M., Graves, J., Zhong, L., and Moreno, S.N. (2001) A plasma membrane-type Ca^{2+}-ATPase co-localizes with a vacuolar H^+-pyrophosphatase to acidocalcisomes of *Toxoplasma gondii*. *EMBO J* **20:** 55–64.

Luo, S., Ruiz, F.A., and Moreno, S.N. (2005) The acidocalcisome Ca^{2+}-ATPase (TgA1) of *Toxoplasma gondii* is required for polyphosphate storage, intracellular calcium homeostasis and virulence. *Mol Microbiol* **55:** 1034–1045.

Lv, S., Zhang, K., Gao, Q., Lian, L., Song, Y., and Zhang, J. (2008) Overexpression of an H^+-PPase gene from *Thellungiella halophila* in cotton enhances salt tolerance and improves growth and photosynthetic performance. *Plant Cell Physiol* **49:** 1150–1164.

McIntosh, M.T., Drozdowicz, Y.M., Laroiya, K., Rea, P.A., and Vaidya, A.B. (2001) Two classes of plant-like vacuolar-type H^+-pyrophosphatases in malaria parasites. *Mol Biochem Parasitol* **114:** 183–195.

Maeshima, M. (2000) Vacuolar H^+-pyrophosphatase. *Biochim Biophys Acta* **1465:** 37–51.

Marchesini, N., Luo, S., Rodrigues, C.O., Moreno, S.N., and Docampo, R. (2000) Acidocalcisomes and a vacuolar

H^+-pyrophosphatase in malaria parasites. *Biochem J* **347** (Part 1): 243–253.
Miranda, K., Pace, D.A., Cintron, R., Rodrigues, J.C., Fang, J., Smith, A., *et al.* (2010) Characterization of a novel organelle in *Toxoplasma gondii* with similar composition and function to the plant vacuole. *Mol Microbiol* **76:** 1358–1375.
Moreno, S.N., and Zhong, L. (1996) Acidocalcisomes in *Toxoplasma gondii* tachyzoites. *Biochem J* **313** (Part 2): 655–659.
Moreno, S.N., Zhong, L., Lu, H.G., Souza, W.D., and Benchimol, M. (1998) Vacuolar-type H^+-ATPase regulates cytoplasmic pH in *Toxoplasma gondii* tachyzoites. *Biochem J* **330** (Part 2): 853–860.
Pace, D.A., Fang, J., Cintron, R., Docampo, M.D., and Moreno, S.N. (2011) Overexpression of a cytosolic pyrophosphatase (TgPPase) reveals a regulatory role of PPi in glycolysis for *Toxoplasma gondii*. *Biochem J* **440:** 229–240.
Park, S., Li, J., Pittman, J.K., Berkowitz, G.A., Yang, H., Undurraga, S., *et al.* (2005) Up-regulation of a H^+-pyrophosphatase (H^+-PPase) as a strategy to engineer drought-resistant crop plants. *Proc Natl Acad Sci USA* **102:** 18830–18835.
Parussini, F., Coppens, I., Shah, P.P., Diamond, S.L., and Carruthers, V.B. (2010) Cathepsin L occupies a vacuolar compartment and is a protein maturase within the endo/exocytic system of *Toxoplasma gondii*. *Mol Microbiol* **76:** 1340–1357.
Patel, S., and Docampo, R. (2010) Acidic calcium stores open for business: expanding the potential for intracellular Ca^{2+} signaling. *Trends Cell Biol* **20:** 277–286.
Pedersen, S.F., Hoffmann, E.K., and Mills, J.W. (2001) The cytoskeleton and cell volume regulation. *Comp Biochem Physiol A Mol Integr Physiol* **130:** 385–399.
Rodrigues, C.O., Scott, D.A., Bailey, B.N., De Souza, W., Benchimol, M., Moreno, B., *et al.* (2000) Vacuolar proton pyrophosphatase activity and pyrophosphate (PPi) in *Toxoplasma gondii* as possible chemotherapeutic targets. *Biochem J* **349** (Part 3): 737–745.
Rohloff, P., Rodrigues, C.O., and Docampo, R. (2003) Regulatory volume decrease in *Trypanosoma cruzi* involves amino acid efflux and changes in intracellular calcium. *Mol Biochem Parasitol* **126:** 219–230.
Rohloff, P., Miranda, K., Rodrigues, J.C., Fang, J., Galizzi, M., Plattner, H., *et al.* (2011) Calcium uptake and proton transport by acidocalcisomes of *Toxoplasma gondii*. *PLoS ONE* **6:** e18390.
Scott, D.A., de Souza, W., Benchimol, M., Zhong, L., Lu, H.G., Moreno, S.N., and Docampo, R. (1998) Presence of a plant-like proton-pumping pyrophosphatase in acidocalcisomes of *Trypanosoma cruzi*. *J Biol Chem* **273:** 22151–22158.
Serrano, A., Perez-Castineira, J.R., Baltscheffsky, M., and Baltscheffsky, H. (2007) H^+-PPases: yesterday, today and tomorrow. *IUBMB Life* **59:** 76–83.
Seufferheld, M., Vieira, M.C., Ruiz, F.A., Rodrigues, C.O., Moreno, S.N., and Docampo, R. (2003) Identification of organelles in bacteria similar to acidocalcisomes of unicellular eukaryotes. *J Biol Chem* **278:** 29971–29978.
Seufferheld, M., Lea, C.R., Vieira, M., Oldfield, E., and Docampo, R. (2004) The H^+-pyrophosphatase of *Rhodospirillum rubrum* is predominantly located in polyphosphate-rich acidocalcisomes. *J Biol Chem* **279:** 51193–51202.
Wetzel, D.M., Chen, L.A., Ruiz, F.A., Moreno, S.N., and Sibley, L.D. (2004) Calcium-mediated protein secretion potentiates motility in *Toxoplasma gondii*. *J Cell Sci* **117:** 5739–5748.
Zhang, J., Li, J., Wang, X., and Chen, J. (2011) OVP1, a vacuolar H^+-translocating inorganic pyrophosphatase (V-PPase), overexpression improved rice cold tolerance. *Plant Physiol Biochem* **49:** 33–38.

Supporting information

Additional supporting information may be found in the online version of this article at the publisher's web-site.